



**Environmental  
Science**  
Nano

**Food-grade titanium dioxide particles decrease the bioaccessibility of iron released from spinach leaves in simulated human gastrointestinal tract**

Journal:	<i>Environmental Science: Nano</i>
Manuscript ID	EN-ART-01-2021-000064.R1
Article Type:	Paper

**SCHOLARONE™**  
Manuscripts

### Environmental Significance

Food-grade titanium dioxide (E171) is widely used as additives in various food products, such as confectionery, sauces, and salad dressings. Up to 36% of E171 particles is in nano-range (< 100 nm). Spinach leaves, the most consumed ingredients of salads globally, are important sources of minerals (e.g., Fe and Ca). Thus, E171 can be co-ingested with spinach leaves. However, knowledge on the potential effect of E171 on spinach leaf digestion and the bioaccessibility of its minerals (Ca, K, Mg, Fe, Mn, Zn, P and S) is very limited. In a simulated human gastrointestinal system, addition of 0.2 wt% E171 reduced the activity of  $\alpha$ -amylase and adsorbed Fe ions released from the leaf digestion, and subsequently decreased the Fe bioaccessibility. Our findings provide important information for the interaction mechanisms of E171 particles with digestive enzymes ( $\alpha$ -amylase, pepsin, pancreatin) during the spinach leaf digestion. The results also shed light on the impact of E171 on the nutritional attributes of foods for human health and wellness.

1  
2  
3 **Food-grade titanium dioxide particles decrease the bioaccessibility of iron**  
4  
5  
6 **released from spinach leaves in simulated human gastrointestinal tract**  
7

8 Chunyang Li<sup>a</sup>, Chuanxin Ma<sup>b, c</sup>, Heping Shang<sup>a</sup>, Jason C. White<sup>c</sup>, David Julian McClements<sup>d</sup>, and  
9  
10 Baoshan Xing<sup>a, \*</sup>  
11

12  
13 <sup>a</sup> Stockbridge School of Agriculture, University of Massachusetts, Amherst, MA 01003, USA  
14

15 <sup>b</sup> Key Laboratory for City Cluster Environmental Safety and Green Development of the Ministry  
16  
17 of Education, Institute of Environmental and Ecological Engineering, Guangdong University of  
18  
19 Technology, Guangzhou 510006, China  
20  
21

22  
23 <sup>c</sup> The Connecticut Agricultural Experiment Station, New Haven, Connecticut 06504, USA  
24

25 <sup>d</sup> Department of Food Science, University of Massachusetts, Amherst, MA 01003, USA  
26

27 \* Corresponding author: Dr. Baoshan Xing (bx@umass.edu)  
28  
29  
30  
31  
32  
33  
34  
35  
36  
37  
38  
39  
40  
41  
42  
43  
44  
45  
46  
47  
48  
49  
50  
51  
52  
53  
54  
55  
56  
57  
58  
59  
60

## Abstract

Food grade titanium dioxide particles (E171) are added to various foods as whitening agents, including chewing gums, candies, sauces, salad dressings, and powdered milks. Salad dressings are often consumed with leafy green vegetables, such as spinach, which are rich in minerals. We hypothesized that the presence of E171 particles in foods would interfere with the bioaccessibility of essential minerals. Therefore, we investigated the impact of E171 on the bioaccessibility of minerals (Ca, K, Mg, Fe, Mn, Zn, P and S) released from spinach leaves using a simulated human digestion tract (GIT) that involves oral, gastric, and small intestinal phases. The digestive enzymes used in the GIT model, including  $\alpha$ -amylase, pepsin, and pancreatin, prompted mineral release from spinach leaves under the simulated GIT conditions (except for Ca). E171 particles did not impact the bioaccessibility of most minerals, except for Fe. The final bioaccessibility of Fe decreased from 59% without E171 to 53% with 0.2 wt% E171. Interestingly, the decrease in Fe bioaccessibility mainly occurred within the oral phase, rather than the gastric or intestinal phases. Mechanistic studies indicated that the reduction in Fe bioaccessibility was due to the following two processes: (i) inhibition of  $\alpha$ -amylase activity by E171, thereby interfering with Fe release from the spinach leaves and (ii) adsorption of Fe onto E171 particles. The results of this study are useful for assessing the potential impact of E171 on the human digestive process and the nutritional value of foods.

**Keywords:** Food grade titanium dioxide particles; iron; minerals; *in vitro* digestion; gastrointestinal tract

## Introduction

Titanium dioxide ( $\text{TiO}_2$ ) particles have been used as an additive in paints, personal care products, and foods.<sup>1</sup> As a food additive, titanium dioxide (E171) has been reported in more than 900 commonly consumed food products, mainly because of its ability to improve their aesthetic properties, especially their appearance.<sup>2</sup> In the USA, the Food and Drug Administration (FDA) limits the use of E171 as a food additive to 1% of the overall food weight.<sup>3</sup> In Europe, E171 can be used in foods at a *quantum satis* level, *i.e.*, the quantity required to achieve the intended purpose.<sup>4</sup>  $\text{TiO}_2$  particles are typically used as whitening or brightening agents because they have a relatively high refractive index and scatter light strongly. They are used for this purpose in numerous foods, including confectionery, dairy products, sauces, salad dressings, and pastries.<sup>5</sup> Their level is particularly high in many candies, with  $\text{TiO}_2$  content reaching 2.5 mg Ti  $\text{g}^{-1}$  of food. It is estimated that the average adult can consume 0.7-5.9 mg of  $\text{TiO}_2$   $\text{kg}^{-1}$  of body weight (BW) per day, and children can consume up to 5 times that of an adult person using this same metric.<sup>6</sup> These studies have highlighted that there may be appreciable levels of E171 in the human diet depending on the nature of the foods consumed.<sup>7</sup>

Spinach, a leafy green vegetable, is one of the most common ingredients of salads consumed worldwide.<sup>8</sup> Its consumption is claimed to have a number of positive biological impacts, including antioxidant, anti-inflammatory, antiproliferative, and anti-obesity effects, which can protect humans against chronic disease.<sup>9</sup> Spinach is also an important source of vitamins, minerals, phenolic compounds, carotenoids, and dietary fibers.<sup>10</sup> Minerals are necessary for the maintenance of certain physiological processes that are essential to human life.<sup>11</sup> Ca, as a cofactor for many enzymes, is also a messenger in intracellular cascade signaling reactions.<sup>12</sup> Fe, Mn, and Zn are cofactors participating in the activity of numerous physiological processes, such as cellular

1  
2  
3 homeostasis and survival, as well as organ and tissue development.<sup>13</sup> Mineral deficiencies are a  
4 worldwide health problem affecting people in developing and some developed countries.<sup>14</sup> It is  
5 estimated that Ca, Zn, and Fe deficiencies lead to health issues in billions of people globally.<sup>15</sup>  
6  
7 Low Zn blood levels may lead to clinical symptoms, including growth retardation, impaired brain  
8 development and cognitive performance, infertility, and increased risk of infections.<sup>16</sup> Fe  
9 deficiency is the major cause of anemia associated with respiratory weakness, as well as abnormal  
10 mental and motor development.<sup>17</sup> Previous studies have focused on the total amount of minerals  
11 present in the food matrix, but this may not provide an inaccurate evaluation of the nutritional  
12 potential of the minerals.<sup>18</sup> The term “bioaccessibility” is defined as nutrients that are released  
13 from the food matrix into the gastrointestinal tract and are available for absorption within the small  
14 intestinal.<sup>19</sup> The low bioaccessibility of minerals in some food products can contribute to  
15 inadequate mineral intake.<sup>20</sup>  
16  
17  
18  
19  
20  
21  
22  
23  
24  
25  
26  
27  
28  
29

30  
31 As mentioned earlier, E171 particles are commonly used as additives in salad dressings to  
32 improve their visual appearance. Salad dressings are designed to be consumed with salads, which  
33 contain leafy greens that are rich in essential minerals. Titanium dioxide is known to interact with  
34 digestive enzymes and minerals (see below). We therefore hypothesized that E171 particles might  
35 impact the bioaccessibility of essential minerals in the leafy greens found in salads.  
36  
37  
38  
39  
40  
41

42 A simulated human gastrointestinal tract (GIT) model, which included oral, gastric, and small  
43 intestinal phases, was used to digest spinach leaves mixed with E171 and to evaluate the effects of  
44 E171 particles on the bioaccessibility of minerals in spinach. In the GIT model, salivary  $\alpha$ -amylase  
45 was included in the oral phase to initialize the digestion of polysaccharides and oligosaccharides.<sup>21</sup>  
46 Pepsin was added in the gastric fluid to degrade proteins by cleaving peptide bonds under acidic  
47 conditions.<sup>22</sup> Pancreatin, a gastrointestinal extract containing  $\alpha$ -amylase, lipase, and proteases, was  
48  
49  
50  
51  
52  
53  
54  
55  
56  
57  
58  
59  
60

1  
2  
3 added to the small intestinal fluid to digest fats, proteins, and carbohydrates.<sup>23</sup> Spinach leaves are  
4 mechanically, chemically, and enzymatically degraded as they pass through each GIT phase,  
5  
6 thereby leading to the release of the minerals into the gastrointestinal fluids. Studies have reported  
7  
8 that the activity of numerous kinds of enzymes are decreased after they adsorb onto the surfaces  
9  
10 of TiO<sub>2</sub> particles, including  $\beta$ -galactosidase, alkaline phosphatase,  $\beta$ -glucosidase, L-leucin, and  
11  
12 aminopeptidase.<sup>24-26</sup> Researchers have also reported that TiO<sub>2</sub> particles significantly decreased  
13  
14 pepsin activity due to particle-enzyme interactions.<sup>27</sup> In addition, several studies have  
15  
16 demonstrated that TiO<sub>2</sub> nanoparticles can interact with heavy metals, including As,<sup>28</sup> Cd,<sup>29</sup> Zn,<sup>29</sup>  
17  
18 <sup>30</sup> and Cu<sup>31</sup> via electrostatic interactions or chemical bonding.<sup>32</sup> Thus, we hypothesized that E171  
19  
20 could decrease mineral bioaccessibility in the GIT model *via* two mechanisms: ( i ) E171 particles  
21  
22 may inhibit enzyme activities (*e.g.*,  $\alpha$ -amylase, pepsin, and pancreatin), thereby reducing the  
23  
24 digestion of the spinach leaves and the release of the minerals; and ( ii ) E171 particles may bind  
25  
26 with the minerals released from the spinach leaves, thereby decreasing mineral bioaccessibility.  
27  
28  
29  
30  
31  
32

33  
34 To test these hypotheses, a mixture of spinach leaves and E171 was passed through the  
35  
36 simulated GIT model and the bioaccessibility of the minerals released from the spinach was  
37  
38 determined. The concentrations of macronutrients (Ca, K, Mg, P, and S) and micronutrients (Fe,  
39  
40 Zn, and Mn) in the digesta from each stage of the GIT model were measured and the  
41  
42 bioaccessibility were then calculated. Mechanistic studies were then carried out using a range of  
43  
44 methods to characterize the nature of any interactions between E171 particles, enzymes, and  
45  
46 minerals. Our results provide useful information about the potential impact of E171 additives on  
47  
48 the human digestive system and the nutritional value of foods.  
49  
50

## 51 **Materials and Methods**

### 52 **Materials**

1  
2  
3 Food-grade TiO<sub>2</sub> particles (E171, purity 99%) were purchased from Precheza (Přerov, Czech  
4 Republic). Baby spinach (Dole fresh, Dole Food Company, Inc, Boston) was purchased from a  
5 local supermarket. Mucin from porcine gastric, bile salts, pepsin from porcine gastric mucosa ( $\geq$   
6 250 units mg<sup>-1</sup>),  $\alpha$ -amylase from porcine pancreas ( $\geq$  10 units mg<sup>-1</sup>), pancreatin from porcine  
7 pancreas (100 - 500 units mg<sup>-1</sup>), and trypsin from porcine pancreas (1000-2000 units mg<sup>-1</sup>), were  
8 purchased from Sigma-Aldrich (St. Louis, MO). All other chemicals or reagents used in this study  
9 were of analytical grade and were purchased from either Sigma-Aldrich or Fisher Scientific.  
10  
11  
12  
13  
14  
15  
16  
17  
18  
19

### 20 **Simulated GIT Model**

21  
22 The simulated GIT model (Table S1 in the Supporting Information, SI), which has been  
23 widely used in a number of previous studies,<sup>33-39</sup> was adopted with some minor modifications. A  
24 1% (w/w) of food grade TiO<sub>2</sub> (E171) particle stock suspension was prepared by adding E171  
25 powder into distilled water, and then sonicating for 15 min using a sonicator (Fisherbrand™ 120  
26 Sonic Dismembrator) to reduce particle agglomeration.  
27  
28  
29  
30  
31  
32

33  
34 Different concentrations of E171 (0, 0.002, 0.05 and 0.2 wt%) were prepared by diluting the  
35 stock E171 suspension in nano-pure water. The concentrations of E171 in the gastrointestinal  
36 system were selected and used based on around 1:2 ratio of a salad dressings (TiO<sub>2</sub> 113 mg per  
37 serving)<sup>5</sup> and spinach leaves (85 g per serving). Fresh spinach leaves were selected and then cut  
38 into 10 mm × 10 mm pieces. Two g of spinach leaves and 13 g of E171 suspensions with different  
39 concentrations were placed in a glass vial containing 15 g of simulated saliva fluid (SSF), in which  
40 the concentrations of mucin and  $\alpha$ -amylase were 3.0 and 0.5 g L<sup>-1</sup>, respectively. The mixture was  
41 adjusted to pH 6.8 and then shaken for 5 min in a shaker maintained at 37 °C to simulate oral  
42 agitation. Then 15 g of oral digesta solution were collected and stored for measuring the amount  
43 of minerals released in the oral phase. An aliquot of simulated gastric fluid (15 g) containing pepsin  
44  
45  
46  
47  
48  
49  
50  
51  
52  
53  
54  
55  
56  
57  
58  
59  
60



1  
2  
3 (3.2 g L<sup>-1</sup>) was then added into the vials. The mixture was then adjusted to pH 2.5 and shaken at  
4  
5 37 °C and 100 rpm to mimic the gastric phase. After a 2-hour incubation, 5 g of gastric digesta  
6  
7 solution were collected and stored in the refrigerator for element concentration determination in  
8  
9 the gastric phase. The remaining sample was then adjusted to pH 7.0 and 5 mL of simulated  
10  
11 intestinal fluid (SIF), which contained pancreatin (14.4 g L<sup>-1</sup>) and bile salts (30 g L<sup>-1</sup>), was added.  
12  
13 The pH was then adjusted to 7.0 and the sample was shaken at 37 °C and 100 rpm to simulate small  
14  
15 intestinal phase. After a 2-hour incubation, the intestinal digesta was collected and stored in the  
16  
17 refrigerator for element concentration determination in the small intestinal phase.  
18  
19  
20

21  
22 To test the adsorption of released minerals onto E171 particles, an identical experiment was  
23  
24 conducted but without the addition of E171. The collected samples at each phase were centrifuged  
25  
26 and then separated into two portions: one portion was used to measure the elemental content in the  
27  
28 absence of E171; the other portion was mixed with suspensions containing different concentrations  
29  
30 of E171 (0.002, 0.05, 0.2 wt%). Briefly, the mixture was shaken for either 5 min or 2 hours to  
31  
32 simulate each phase. After incubation, a sample of digesta solution (1 or 2 g) was collected from  
33  
34 oral, gastric, and small intestinal phases for ICP-OES measurement. The amount of minerals  
35  
36 adsorbed onto the E171 particles was determined by the differences between the two  
37  
38 corresponding portions.  
39  
40  
41

#### 42 **Element Measurement by ICP-OES**

43

44  
45 The samples collected from each phase were passed through the simulated GIT tract and then  
46  
47 centrifuged at 4000 rpm for 30 min. The supernatant was used to measure the concentration of  
48  
49 macronutrients (Ca, K, Mg, P, S) and micronutrients (Fe, Mn, Zn) released from the spinach leaves  
50  
51 in the oral, gastric, and small intestinal phase. The supernatants and leaf debris collected from each  
52  
53 phase were digested with HNO<sub>3</sub> at 115 °C for 40 min. The digesta were diluted to 15, 20 and 30  
54  
55  
56  
57  
58  
59  
60

1  
2  
3 mL using deionized water for oral, gastric, and small intestinal phases, respectively. Inductively  
4  
5 coupled plasma optical emission spectrometry (ICP-OES, iCAP 6500, Thermo Fisher Scientific,  
6  
7 Waltham, MA) was used to measure the element concentrations. The bioaccessibility of the  
8  
9 minerals in each phase was calculated as follows<sup>40</sup>:

$$\text{Bioaccessibility (\%)} = \text{mineral in collected supernatant (\mu g)} / \text{total mineral (\mu g)} \times 100$$

### 14 **UV-visible spectroscopy measurements**

15  
16  
17 The amounts of digestive enzymes that had adsorbed to the surfaces of E171 particles were  
18  
19 determined using UV-visible spectroscopy.

20  
21  *$\alpha$ -Amylase*: Initially, a standard curve ( $r^2 = 0.9999$ ) of  $\alpha$ -amylase was prepared by diluting  
22  
23 amylase stock solution ( $5 \text{ mg mL}^{-1}$ ) to different concentrations ranging from 0 to  $3 \text{ mg mL}^{-1}$  in  
24  
25 simulated saliva solution. The absorbance of these solutions was then measured at 260 nm using a  
26  
27 UV-Vis spectrophotometer.<sup>41</sup> The interactions between E171 and  $\alpha$ -amylase were assessed by  
28  
29 mixing 1.5 mL of E171 suspensions ( $0, 0.2, 1, 2, 5, 20 \text{ mg mL}^{-1}$ ) with 1.5 mL of  $\alpha$ -amylase solution  
30  
31 ( $5 \text{ mg mL}^{-1}$ ). The resulting mixtures (pH 6.8) were then shaken at  $37 \text{ }^\circ\text{C}$  for 5 min prior to  
32  
33 measurement. After centrifugation, the concentration of non-adsorbed  $\alpha$ -amylase remaining in the  
34  
35 solution was then determined from the calibration curve.

36  
37  
38  
39  
40 *Pepsin*: To establish a calibration curve, pepsin stock solution ( $1.6 \text{ mg mL}^{-1}$ ) was diluted with  
41  
42 gastric solution (NaCl-HCl) to make a series of different concentrations ( $0\text{-}1.6 \text{ mg mL}^{-1}$ ) of pepsin,  
43  
44 and the absorbance of each calibration point was recorded at 296 nm ( $r^2 = 0.9996$ ). The enzyme-  
45  
46 E171 interactions were assessed by mixing 1.5 mL of E171 suspension ( $0, 0.02, 0.1, 0.2, 0.5, 1, 2$   
47  
48  $\text{mg mL}^{-1}$ ), 1.5 mL of saliva solution (without  $\alpha$ -amylase) and 3.0 mL of pepsin solution ( $3.2 \text{ mg}$   
49  
50  $\text{mL}^{-1}$ ) at pH 2.5 and then shaking at  $37 \text{ }^\circ\text{C}$  for 2 hours. The resulting mixture was centrifuged at  
51  
52  
53  
54  
55  
56  
57  
58  
59  
60

1  
2  
3 4000 rpm for 15 min. The amount of pepsin in the supernatant was then determined by measuring  
4  
5 the absorbance at 296 nm.<sup>42</sup>  
6

7  
8 *Pancreatin*: A calibration curve was prepared by diluting pancreatin stock solution (1.8 mg  
9 mL<sup>-1</sup>) to different concentrations ranging from 0 to 0.6 mg mL<sup>-1</sup> in SIF solution (pH 7.0) and then  
10 the absorbance was measured at 260 nm using a UV-visible spectrometer ( $r^2 = 0.9995$ ). The  
11 pancreatin-E171 interactions were then assessed by mixing 1.5 mL of E171 suspension (0, 0.0025,  
12 0.0125, 0.025, 0.0625, 0.125, or 0.25 mg mL<sup>-1</sup>), 1.5 mL of salivary solution (without  $\alpha$ -amylase),  
13 and 3.0 mL of gastric solution (without pepsin) and then adjusting the system to pH 7.0. Then, 1.2  
14 mL of small intestinal solution containing pancreatin (1.8 mg mL<sup>-1</sup>) was added to this mixture and  
15 the pH was adjusted to 7.0 again. The total system was then incubated in shaker at 37 °C for 2  
16 hours. After centrifugation, the amount of pancreatin in the supernatant was determined from the  
17 calibration curve by measuring the absorbance at 260 nm.  
18  
19  
20  
21  
22  
23  
24  
25  
26  
27  
28  
29

### 30 **Enzymatic Activity Assay ( $\alpha$ -amylase, pepsin, and pancreatin)**

31  
32  
33  *$\alpha$ -Amylase*: The  $\alpha$ -amylase activity was measured as described in Jiang et al.<sup>35</sup> and Terra et  
34 al.<sup>43</sup> The method used was based on the quantification of the reducing sugars released from the  
35 starch hydrolysis reaction, which is catalyzed by  $\alpha$ -amylase. The calculation details for  $\alpha$ -amylase  
36 activity are described in Experiment S2. A 1% (w/v) soluble starch solution was prepared by  
37 dissolving 1.0 g soluble starch into 100 mL boiling buffer solution (20 mM sodium phosphate, 6.7  
38 mM sodium chloride, pH 6.9). A series of concentrations of E171 (0, 0.006, 0.031, 0.062, 0.154,  
39 0.308, or 0.615 mg mL<sup>-1</sup>) were separately mixed with an equal volume (0.5 mL) of  $\alpha$ -amylase  
40 solution (2 unit) at pH 6.8 (by adding 12  $\mu$ L 0.1N NaOH and 20  $\mu$ L 0.01N NaOH) and shaken at  
41 37 °C for 5 mins. Afterwards, 1 mL of 1.0 % (w/v) soluble starch solution was added into a tube  
42 containing the above mixture. After incubation in a shaker at 37 °C for exact 3 min, the reaction  
43  
44  
45  
46  
47  
48  
49  
50  
51  
52  
53  
54  
55  
56  
57  
58  
59  
60

1  
2  
3 was terminated by adding 1 mL of color reagent solution (20 mL of 96 mM 3,5-Dinitrosalicylic  
4 acid solution, 8 mL of 5.3 M potassium sodium tartrate, tetrahydrate solution in 2 M NaOH  
5 solution, 12 mL of DI water) into the final product and then all tubes were placed into hot water  
6 (90 °C) for 15 min. After cooling to room temperature, 9 mL of deionized water were added into  
7 each tube and mixed thoroughly. After centrifugation (4000 rpm, 15 min), the concentration of  
8 maltose in the supernatant was then measured at 540 nm.  
9  
10  
11  
12  
13  
14  
15

16  
17 *Pepsin:* The method used to determine pepsin activity was based on that of Zhu et al. with  
18 some minor modifications.<sup>27</sup> Pepsin can convert hemoglobin to tryptophan and tyrosine, both of  
19 which are easily detected at 280 nm by UV-vis spectrophotometry. The calculation details for  
20 pepsin activity are described in Experiment S3. Samples were prepared by mixing 187.5 µL of  
21 E171 suspension (0, 0.002, 0.01, 0.02, 0.05, 0.1, or 0.2 mg mL<sup>-1</sup>), 187.5 µL of saliva solution  
22 (without α-amylase) and 375 µL of pepsin solution (0.32 mg mL<sup>-1</sup>) and then adjusting to pH 2.5  
23 (by adding 2 µL 6 N NaOH and 16 µL 1 N NaOH) and shaking at 37 °C for 30 min. Then, 750 µL  
24 of pepsin-E171 mixture were incubated with 3.75 mL of bovine hemoglobin solution (5 mg mL<sup>-1</sup>)  
25 at 37 °C. After 30 min, 7.5 mL of 5% (w / v) trichloroacetic acid were added into the mixture to  
26 stop the reaction and the sample was shaken for another 10 min at 37 °C. After centrifugation, the  
27 supernatant was measured at 280 nm. The inhibition rate of α-amylase and pepsin as affected by  
28 E171 was calculated as the percentage of the control<sup>41</sup>:  
29  
30  
31  
32  
33  
34  
35  
36  
37  
38  
39  
40  
41  
42  
43  
44

$$\% \text{ Inhibition rate} = [1 - (\text{OD of test} / \text{OD of control})] \times 100$$

45  
46

47 *Trypsin:* Trypsin, rather than pancreatin, was used in this experiment to determine the impact  
48 of E171 on enzyme activity in the small intestinal phase. This was done to simplify interpretation  
49 of the results since pancreatin contains a complex mixture of different enzymes. Trypsin activity  
50 was measured using a vendor-supplied (Sigma) method with some modifications. N<sub>α</sub>-Benzoyl-L-  
51  
52  
53  
54  
55  
56  
57  
58  
59  
60

1  
2  
3 arginine ethyl ester (BAEE), the final product of the reaction, was used to determine trypsin  
4 activity. A mixture containing 0.5 mL of E171 suspension (0 or 0.278 mg mL<sup>-1</sup>), 0.5 mL of saliva  
5 solution, 1.0 mL of gastric solution and 0.4 mL of trypsin (2 mg mL<sup>-1</sup>) was incubated at pH 7.0,  
6 37 °C for 10 min. After centrifugation, 1.2 mL of supernatant was immediately mixed with 2.0 mL  
7 of BAEE (0.13 mg mL<sup>-1</sup>). The increase in absorbance at 253 nm was recorded for 5 min at 1 min  
8 intervals. The rate in the increase of the absorbance ( $\Delta A_{253} \text{ min}^{-1}$ ) was then used to calculate the  
9 amount of BAEE produced (unit mL<sup>-1</sup>).  
10  
11  
12  
13  
14  
15  
16  
17  
18

### 19 **FTIR Spectroscopy**

20  
21 The FTIR spectra of E171,  $\alpha$ -amylase, pepsin, pancreatin, E171+ $\alpha$ -amylase, E171+pepsin,  
22 and E171+pancreatin were recorded using a PerkinElmer Spectrum instrument (USA) that was  
23 operated in the attenuated total reflection (ATR) mode at a resolution of 4 cm<sup>-1</sup>. Samples of  
24 E171+ $\alpha$ -amylase, E171+pepsin, and E171+pancreatin were collected from the oral phase (pH 6.8,  
25 37 °C, 5 mins), gastric phase (pH 2.5, 37 °C, 2 hours), and small intestinal phase (pH 7.0, 37 °C, 2  
26 hours), respectively. The supernatants of these samples were collected after centrifugation. The  
27 target compounds, including E171+ $\alpha$ -amylase, E171+pepsin, and E171+pancreatin, were rinsed  
28 three times with the corresponding buffer solution (saliva fluid, gastric solution, intestinal fluid,  
29 respectively). The collected samples were re-suspended in the corresponding solutions for FTIR  
30 spectra analysis. Each spectrum was collected over the range from 4000 to 500 cm<sup>-1</sup> with 200 scans.  
31 The final spectra of each sample were an average of three replicates.  
32  
33  
34  
35  
36  
37  
38  
39  
40  
41  
42  
43  
44  
45  
46

### 47 **Fluorescence Spectroscopy**

48  
49 Fluorescence spectroscopy was used to investigate the impact of E171 concentration (0, 1, 2,  
50 4, 6, 8, 10 mg L<sup>-1</sup>) on the spectra/availability of digestive enzymes ( $\alpha$ -amylase and pepsin) to  
51 provide some insights into binding interactions. Mixtures of 1.5 mL of  $\alpha$ -amylase (150 mg L<sup>-1</sup>)  
52  
53  
54  
55  
56  
57  
58  
59  
60

1  
2  
3 and 1.5 mL of E171 suspension (pH 6.8) were shaken and incubated at 37 °C for 5 min. For pepsin,  
4  
5 3 mL of pepsin solution (75 mg L<sup>-1</sup>) was mixed with 1.5 mL of saliva fluid (only ions) and 1.5 mL  
6  
7 of E171 suspension (pH 2.5), and then the mixture was shaken and incubated at 37 °C for 2 hours.  
8  
9  
10 The fluorescence emission spectra of all samples were excited at 280 nm and recorded from 300  
11  
12 to 500 nm using a fluorescence spectrophotometer (Hitachi, Ltd., Japan). Since blank E171 also  
13  
14 exhibited detectable signals, which can interfere with fluorescence intensity of enzymes, the  
15  
16 intensity of fluorescence used was corrected by subtracting emission spectra of the corresponding  
17  
18 E171 solution from that of E171-enzymes. Fluorescence quenching was described by the Stern-  
19  
20 Volmer's equation as follows<sup>41</sup>:  
21  
22

$$F_0/F = 1 + K_{sv}[Q] = 1 + K_q\tau_0[Q]$$

23  
24  
25  
26 Where,  $F_0$  and  $F$  represent the fluorescence intensities in the absence and presence of E171,  
27  
28 respectively;  $[Q]$  is the concentration of the quencher (E171);  $K_{sv}$  is the Stern-Volmer quenching  
29  
30 constant;  $K_q$  is the bimolecular quenching constant; and  $\tau_0$  is the lifetime of the fluorophore (for  
31  
32 tryptophan,  $\tau_0$  is 5.7 ns). In addition, the interaction between the quencher and enzyme was  
33  
34 described using the Scatchard equation<sup>44</sup>:  
35  
36

$$\text{Log}((F_0-F)/F) = \log K_a + n \log[Q]$$

37  
38  
39 where,  $K_a$  is the binding constant associated with the E171-enzyme interactions and  $n$  is the  
40  
41 number of binding sites.  
42  
43

#### 44 **Statistical analysis**

45  
46  
47 All experiments were conducted at least in triplicate. Significant differences between  
48  
49 treatment groups were determined by an analysis of ANOVA with Sidak's test on OriginPro 2018  
50  
51 statistical software (OriginLab Corp., USA). We used  $p < 0.05$  for being statistically significant.  
52  
53

#### 54 **Results and Discussion**

### Impact of digestive enzymes on mineral bioaccessibility

Digestive enzymes (amylase, pepsin, and pancreatin) significantly increased mineral bioaccessibility in spinach leaves, except for Ca (Figure 1 and S1). For most of the minerals, more than 60% was released after passing through the simulated GIT model. In the absence of the digestive enzymes, only about 40% of K, Mg, Zn, and Mn were released, and about 20% of P, S, and Fe were released. These results demonstrate the critical role of digestive enzymes in breaking down plant tissue structure in the spinach leaves to release minerals. In the oral phase,  $\alpha$ -amylase can catalyze the hydrolysis of internal  $\alpha$ -1,4-glycosidic linkages in polysaccharides into glucose, maltose, and maltotriose units.<sup>45</sup>  $\alpha$ -Amylases act on starch, glycogen, and related polysaccharides or oligosaccharides in a random manner.<sup>45</sup> It is noted that spinach does not contain much starch. In addition to constituents of cellulose in the cell wall, other sources of polysaccharides and oligosaccharides are the vacuoles and plastids of plant cells in leafy vegetables.<sup>46</sup> Thus,  $\alpha$ -amylase may still hydrolyze polysaccharides or oligosaccharides within vacuoles and plastid of the plant-tissue matrix to facilitate mineral release. This could explain the observation that the addition of amylase significantly increased the bioaccessibility of K, Mg, Mn, Zn, Fe, P, and S from 1.52- to 7.08-fold compared to the corresponding blank. In the gastric phase, pepsin, which degrades proteins, had no impact on Ca, K, Mg, Mn, and Zn but significantly increased the bioaccessibility of Fe, P, and S by 1.25- to 2.47-fold. According to their biochemical function, K, Mg, and Mn ions are known to establish cell turgor and maintain cell electroneutrality, while Fe, P, and S are essential constituents of many proteins in tissues.<sup>47</sup> Consequently, pepsin may have hydrolyzed the proteins and facilitated the release of these minerals under simulated gastric conditions. In the small intestinal phase, the presence of pancreatin that can digest fats, proteins, and carbohydrates<sup>23</sup>

1  
2  
3 significantly elevated the bioaccessibility of K, Mg, Mn, Zn, Fe, P, and S by 5.17- to 19.43-fold.  
4  
5 Thus, these enzymes may have facilitated spinach leaf digestion and mineral release.  
6

7  
8 It is noted that the final bioaccessibility of Ca in the spinach leaves was only around 10% after  
9  
10 passing through the full simulated GIT model, even in the presence of digestive enzymes (Figure  
11  
12 1A and S1). Ca bioaccessibility was significantly lower than other minerals that had at least 20%  
13  
14 bioaccessibility. A possible explanation is that Ca is a constituent of the middle lamella of cell  
15  
16 walls<sup>47</sup>, and the upper GIT digestive enzymes used could not digest cellulose, hemicellulose, or  
17  
18 pectin, which are important structural components in primary cell walls. The measured  
19  
20 bioaccessibility (0.3-5%) of Ca in spinach was quite low compared to reported values for its  
21  
22 bioaccessibility in kale and wheat.<sup>48</sup> This may have occurred because spinach contains relatively  
23  
24 high levels of oxalate, which can bind Ca and reduce its bioaccessibility and absorption.<sup>49</sup> All these  
25  
26 results suggest that digestive enzymes can facilitate the breakdown of spinach leaves, which  
27  
28 enhances the release of some minerals. However, the extent of enhancement depends on the  
29  
30 characteristics and location of the minerals within the plant tissues.  
31  
32  
33

### 34 35 **Impact of titanium dioxide on mineral bioaccessibility**

36  
37 The final Fe bioaccessibility decreased significantly from 59% without E171 to 53% in the  
38  
39 presence of 0.2 wt% E171 after passing through the simulated GIT model (Figure 1D).  
40  
41 Interestingly, in the presence of E171, an appreciable decrease in Fe bioaccessibility was evident  
42  
43 in the oral phase rather than the gastric and intestinal phase. Specifically, in the oral phase, samples  
44  
45 containing 0.2 wt% E171 significantly decreased Fe and Zn bioaccessibility by 11% and 6%,  
46  
47 respectively; samples containing 0.05 wt% E171 significantly decreased Fe bioaccessibility by 5%  
48  
49 compared to controls. E171 could decrease mineral bioaccessibility via two pathways: first, E171  
50  
51 could interact with enzymes and reduce the enzymatic activities, thereby inhibiting mineral release  
52  
53  
54  
55  
56  
57  
58  
59  
60



1  
2  
3 from spinach leaves. However, exposure to different concentrations of E171 (0-0.2 wt%) had no  
4 impact on the bioaccessibility of other minerals. In addition, some elements released from spinach  
5 leaves were independent or only slightly dependent on enzyme additions. Thus, even though E171  
6 reduced the enzymatic activity in the specific phase, E171 particles were unlikely to decrease  
7 mineral bioaccessibility via inhibiting these elements released from spinach. The amount of  
8 minerals released from spinach varied, ranging from 10-79% in the presence of digestive enzymes,  
9 with Ca having the lowest and P the highest (Figure 1). The release extent of minerals was distinct  
10 because of their characteristics and locations within plant tissues. As shown in Table S2, the  
11 released minerals from spinach as affected by digestive enzymes can be separated into three levels  
12 by their bioaccessibility as compared to the blank. Level one is no change in the mineral  
13 bioaccessibility as affected by enzymes. For instance, the total bioaccessibility of Ca was only 10%  
14 in all three phases across all the treatments, and most of Ca has remained in the spinach residues.  
15 The bioaccessibility of K, Mg, Mn, and Zn was not affected by pepsin in the gastric phase relative  
16 to the blank. Level two is a minor increase (3-5%) in the mineral bioaccessibility as affected by  
17 enzymes. In the oral phase, K, Mg, and Mn bioaccessibility was 7-10% in the absence of amylase,  
18 but the presence of amylase only increased their bioaccessibility by 3-5%. In the gastric phase, the  
19 bioaccessibility of Fe and P was 18 and 14%, respectively, in the absence of pepsin, and increased  
20 by 4-5% by adding pepsin. Level three is a large increase (12-22%) in the mineral bioaccessibility  
21 as affected by enzymes. For example, in the oral phase, P, S, and Fe bioaccessibility with amylase  
22 were increased by 18-22% compared to the one without amylase. In the gastric phase, S  
23 bioaccessibility with pepsin was increased by 22%. Digestive enzymes can break the structure of  
24 food and subsequently release the elements involved in structural integrity and composition of  
25 carbon compounds, i.e., P and S can be initially released from spinach leaves. In the simulated  
26  
27  
28  
29  
30  
31  
32  
33  
34  
35  
36  
37  
38  
39  
40  
41  
42  
43  
44  
45  
46  
47  
48  
49  
50  
51  
52  
53  
54  
55  
56  
57  
58  
59  
60

1  
2  
3 GIT model, the concentration of E171 was gradually decreased, resulting in less interaction  
4 between E171 and enzymes overtime. Particularly, in the small intestinal phase, although the  
5 addition of pancreatin notably increased the bioaccessibility of all the minerals (except Ca) by over  
6 12-34% as compared to the one without pancreatin, E171 addition showed the insignificant change  
7 in the bioaccessibility of these elements, which could be ascribed as no inhibitory effects of E171  
8 on the pancreatin activity. Thus, it is necessary to investigate the interaction between E171 and  $\alpha$ -  
9 amylase, pepsin, and pancreatin, as well as the inhibitory effects of E171 on enzymatic activities  
10 in the specific phase as discussed below. Also, E171 could decrease Fe bioaccessibility via the  
11 second pathway: the free Fe released from spinach leaves could adsorb on E171 particles. We  
12 therefore further investigated the adsorption of free elements released from spinach leaves onto  
13 E171 particles in the simulated GIT model.  
14  
15  
16  
17  
18  
19  
20  
21  
22  
23  
24  
25  
26  
27

### 28 **Adsorption of minerals onto titanium dioxide particles**

29  
30  
31 To examine the potential cause of the observed decrease in Fe bioaccessibility in the presence  
32 of E171, mineral adsorption onto E171 particles was measured (Table 1). At 0.002 wt% E171, no  
33 mineral adsorption was observed in any of the three GIT phases, suggesting that this low  
34 concentration of E171 particles did not lead to significant mineral adsorption. Additionally, a  
35 common finding in the gastric phase is that no mineral sorption across all the treatments, except S  
36 in the 0.2 wt% E171 treatment. E171 particles adsorbed a minor amount (less than 5%) of elements,  
37 i.e., Ca, Mg, Fe, Mn, Zn, P, and S, in the oral, gastric, or small intestinal phase, but no K adsorption  
38 was observed in all three stages regardless of E171 doses. Divalent cations have been reported to  
39 bind stronger to the nanoparticles surface than monovalent cations.<sup>50</sup> Thus, in the presence of other  
40 elements, K ions were likely outcompeted, leading to minimal change in the K bioaccessibility.  
41  
42  
43  
44  
45  
46  
47  
48  
49  
50  
51  
52  
53  
54  
55  
56  
57  
58  
59  
60

1  
2  
3 phase, respectively. While the amount of Fe, Mn, Zn, and S adsorbed onto E171 ranged from 1 to  
4  
5 5%, in the oral phase, 0.2 wt% E171 adsorbed 5.3% Fe, 4.47% Mn, 3.66% Zn and 1.26% S, as  
6  
7 well as 0.05 wt% E171 adsorbed 3.02% Fe, 1.41% Mn and 1.60% Zn; in the small intestinal phase,  
8  
9 4.01% Mn and 4.27% Zn were adsorbed in the presence of 0.2 wt% E171, respectively. These  
10  
11 results suggest that E171 addition above 0.05 wt% should result in around 1-5% decrease in the  
12  
13 bioaccessibility of Fe, Mn, Zn, and S in the specific phase. However, no significant difference in  
14  
15 mineral bioaccessibility was evident, except for Fe. In the experiment for the bioaccessibility of  
16  
17 minerals as affected by E171, when the minerals were gradually released from spinach by digestive  
18  
19 enzymes, part of the enzymes was already adsorbed onto E171 (see discussion below), then free  
20  
21 minerals were adsorbed onto E171. In the adsorption experiment of minerals by E171 was used to  
22  
23 demonstrate whether E171 additions could decrease the amount of free minerals released from  
24  
25 spinach. The spinach samples were firstly digested in the simulated GIT model, and then in each  
26  
27 phase, a fraction of the digest was used to interact with different concentrations of E171. In this  
28  
29 case, free minerals and enzymes could simultaneously interact with E171. Hence, the decreased  
30  
31 amount of released minerals from adsorption by E171 could be overestimated. Part of the decrease  
32  
33 can be attributed to the binding of Fe to the surface of E171, while this cannot entirely explain the  
34  
35 observed reduction. Thus, it is necessary to further explore whether E171 could exhibit inhibitory  
36  
37 effects on enzymatic activities, leading to inhibition in mineral releases from spinach leaves.

#### 44 **Adsorption of enzymes onto titanium dioxide particles**

45  
46  
47  *$\alpha$ -Amylase*: As the E171-to-amylase ratio increased, the absorbance of amylase decreased (Figure  
48  
49 2A), suggesting that amylase bound to the surface of E171 particles in the oral phase, thereby  
50  
51 leading to a reduction in the amount of free  $\alpha$ -amylase in the supernatant. The amylase  
52  
53 concentration in the supernatant was closely related to the initial concentration ratio (E171-to-  
54  
55  
56  
57  
58  
59  
60

1  
2  
3 amylase) with  $R^2 = 0.88$  (Figure 2B). The  $\zeta$ -potential of E171 and  $\alpha$ -amylase in the oral phase was  
4  
5 -37 and -20 mV, respectively (Figure S2); consequently, one would not expect an electrostatic  
6  
7 attraction between them. However, proteins are known to bind to the surface of inorganic  
8  
9 nanoparticles due to other interactions, such as van der Waals, hydrophobic, or hydrogen bonding  
10  
11 interactions. Thus, we used FTIR to examine the potential binding of the digestive enzymes to  
12  
13 E171 since this technique has previously been shown to be useful for this type of analysis.<sup>51</sup> The  
14  
15 FTIR spectra of E171,  $\alpha$ -amylase, and E171+ $\alpha$ -amylase in the oral phase are shown in Figure 3A.  
16  
17 A broad peak at  $3400\text{ cm}^{-1}$  and a clear peak at  $1640\text{ cm}^{-1}$  were observed in the E171 spectra, which  
18  
19 were assigned to O-H stretching and bending modes.<sup>52</sup> Some characteristic peaks were observed  
20  
21 in the spectra of  $\alpha$ -amylase that were in agreement with those reported in previous studies (Table  
22  
23 S3).<sup>53</sup> The strong and broad peak at  $3400\text{ cm}^{-1}$  was due to the N-H and O-H stretching vibrations.<sup>54</sup>  
24  
25 A slight and clear peak at  $2910\text{ cm}^{-1}$  was attributed to C-H stretching because of methylene.<sup>53</sup> The  
26  
27 band at  $1637\text{ cm}^{-1}$  (amide I) corresponds to C=O stretching vibrations of the peptide bonds.<sup>55</sup>  
28  
29 The broad absorption bands in the range of  $1413$  and  $1258\text{ cm}^{-1}$  refer to amide II and III,  
30  
31 respectively.<sup>53</sup> The other peaks at  $1042$  and  $1038\text{ cm}^{-1}$  may be ascribed to the stretching and  
32  
33 bending vibrations of aliphatic amines.<sup>53</sup> Thus, the appearance of characteristic bands of  $\alpha$ -amylase  
34  
35 at approximately  $2910$ ,  $1404$ ,  $1067$ , and  $1032\text{ cm}^{-1}$  in the spectra of E171+ amylase indicate the  
36  
37 adsorption of  $\alpha$ -amylase to the E171 surface.  
38  
39  
40  
41  
42  
43  
44

45 *Pepsin*: A characteristic absorption peak in the UV-visible spectrum at  $269\text{ nm}$  arose from the  
46  
47  $\pi$ - $\pi^*$  transition in the benzene rings of Trp, Tyr, Phe residues in pepsin.<sup>42</sup> The intensity of the peak  
48  
49 decreased with increasing E171 concentrations (Figure 2C), which can be attributed to enzyme  
50  
51 binding to E171. These results are supported by a previous study suggesting the adsorption of  
52  
53 pepsin onto E171 particles.<sup>27</sup> The pepsin concentration in the supernatant was negatively correlated  
54  
55  
56  
57  
58  
59  
60

1  
2  
3 with the E171-to-pepsin ratio ( $R^2 = 0.99$ , Figure 2D), indicating that increasing additions of E171  
4 reduced the amount of pepsin in the supernatant. The FTIR spectra of E171, pepsin, and  
5 E171+pepsin in the small intestinal phase is shown in Figure 3B. The broad peak observed at 3277  
6  $\text{cm}^{-1}$  in the FTIR spectra of pepsin corresponds to amide A, associated with N-H stretching and  
7 hydrogen bonding; the peak at 2935  $\text{cm}^{-1}$ , referred to as amide B, is from an asymmetrical stretch  
8 of  $\text{CH}_2$  (Table S3).<sup>56</sup> The peaks at 1661  $\text{cm}^{-1}$  and 1537  $\text{cm}^{-1}$ , corresponding to amide I and amide  
9 II groups, respectively, can be attributed to N-H in-plane bending coupled with C=N stretch  
10 bending.<sup>56</sup> The peaks at 1413 and 1233  $\text{cm}^{-1}$  can be ascribed to the amide III groups. The absorption  
11 band of the amide group at 1558  $\text{cm}^{-1}$  in the spectrum of E171+pepsin compared to the spectrum  
12 of E171 indicates the adsorption of pepsin onto the E171 surfaces.

13  
14  
15  
16  
17  
18  
19  
20  
21  
22  
23  
24  
25  
26  
27 *Pancreatin*: No significant differences in pancreatin concentration were evident across all the  
28 E171-to-pancreatin ratios used (0–0.139), suggesting that no adsorption of this enzyme onto the  
29 surfaces of the E171 particles in the small intestinal phase (Figure 2E). The FTIR spectrum of  
30 pancreatin+E171 showed no characteristic peaks of pancreatin, which further confirms the lack of  
31 interaction. Given that pancreatin is a mixture of  $\alpha$ -amylase, lipase, and proteases, this result is  
32 surprising since both  $\alpha$ -amylase and pepsin were shown to bind to E171 in the oral and gastric  
33 phases. It is possible because the E171 concentration was considerably reduced in the small  
34 intestinal due to dilution with the simulated oral, gastric, and intestinal fluids.

### 45 **Effect of titanium dioxide particles on enzymatic activity**

46  
47  
48 Measurements of enzyme activity showed that E171 exhibited inhibition of  $\alpha$ -amylase and  
49 pepsin in the oral and gastric phases, respectively (Figure 3D and E). The degree of inhibition for  
50 both  $\alpha$ -amylase and pepsin increased in a dose-dependent manner. For example, the activity of  $\alpha$ -  
51 amylase decreased from 5.72 to 3.99  $\text{U mL}^{-1}$  when the E171 concentration was increased from 0  
52  
53  
54  
55  
56  
57  
58  
59  
60

1  
2  
3 to 0.615 mg mL<sup>-1</sup>. Jiang et al. reported that both spherical and polygonal starch nanoparticles  
4 (SNPs) inhibited  $\alpha$ -amylase activity in phosphate buffer solution (pH 5.8); mechanistically, the  
5 SNPs interacted with the active site of the  $\alpha$ -amylase, thereby inhibiting its ability to interact with  
6 soluble starch molecules.<sup>41</sup> However, some minerals as ionic forms in plant tissues, e.g., Ca, K,  
7 Mg, and Mn, showed no change or minor increase in their bioaccessibility by adding  $\alpha$ -amylase.  
8 In addition, minerals such as P and S are essential in structural integrity or part of carbon  
9 compounds, which could be easily accessible to  $\alpha$ -amylase than Fe and Zn, which are constituents  
10 of protein interior of plant tissues.<sup>47</sup> Although E171 inhibited 35% of amylase activity, the  
11 remaining amylase could still break down spinach and prompt the releases of these minerals except  
12 Fe and Zn. As mentioned earlier, the bioaccessibility of Fe and Zn in the oral phase decreased  
13 significantly in the presence of E171 particles, *i.e.*, by 11% and 6%, respectively, for 0.2 wt%  
14 E171 (Figure 1D). Part of this decrease can be attributed to the binding of Fe and Zn to the surface  
15 of E171, *i.e.*, by 5% and 4% for 0.2 wt% E171 (Table 1), but this does not fully account for the  
16 observed reduction. Hence, it is possible that part of the observed decrease in Fe and Zn  
17 bioaccessibility was due to the ability of the E171 to decrease the activity of important digestive  
18 enzymes, thereby reducing the amount of minerals released.

19  
20  
21  
22  
23  
24  
25  
26  
27  
28  
29  
30  
31  
32  
33  
34  
35  
36  
37  
38  
39  
40 The enzyme activity of pepsin decreased from 62.37 to 34.74 U mL<sup>-1</sup> as the E171  
41 concentration was increased from 0 to 0.2 mg mL<sup>-1</sup>. Others have also reported that E171 particles  
42 can significantly inhibit pepsin activity.<sup>57</sup> Interestingly, although the addition of 0.2 wt% E171  
43 inhibited pepsin activity, no significant difference in mineral bioaccessibility was observed for any  
44 of the samples in the gastric phase. Among these minerals, the bioaccessibility of Ca, K, Mg, Mn,  
45 and Zn was not affected by the pepsin addition; the bioaccessibility of Fe and P without pepsin  
46 was 14% and 18%, respectively, and only increased by 3-5% with pepsin; S bioaccessibility  
47  
48  
49  
50  
51  
52  
53  
54  
55  
56  
57  
58  
59  
60

1  
2  
3 exhibited a larger increase (8% to 20%) after adding enzyme. These results suggesting that there  
4 was still sufficient pepsin remaining to digest protein and release the three elements in the gastric  
5 phase. Besides, the gastric phase is a strongly acidic environment where spinach leaves could  
6 readily release these minerals as determined by the bioaccessibility of all minerals that were  
7 substantially higher than the other two phases without the addition of enzymes. No significant  
8 difference was found in BAEE concentration between the two E171-to-trypsin ratios used (Figure  
9 3F), suggesting that E171 had no impact on trypsin activity. This result is consistent with the  
10 findings of the bioaccessibility experiment, which showed that E171 concentration did not impact  
11 mineral bioaccessibility in the small intestinal phase.  
12  
13  
14  
15  
16  
17  
18  
19  
20  
21  
22

23  
24 These results suggest that E171 addition may have an inhibitory effect on  $\alpha$ -amylase activity  
25 in the oral phase, thereby impeding the release of minerals from the spinach leaves. It is known  
26 that both the conformation and microenvironment of enzymes play a crucial role in determining  
27 their catalytic efficiency.<sup>58</sup> The adsorption of enzymes onto the surface of E171 particles may have  
28 promoted conformational changes due to alterations in the new microenvironment.<sup>59</sup> For this  
29 reason, fluorescence spectroscopy was used to further explore the inhibitory effect of E171 on  
30 digestive enzyme activity.  
31  
32  
33  
34  
35  
36  
37  
38  
39

### 40 **Fluorescence Analysis**

41  
42 Fluorescence spectroscopy is a powerful tool to obtain information about the  
43 microenvironment of the tryptophan groups in proteins by monitoring changes in their intrinsic  
44 fluorescence intensity.<sup>60</sup> We used this method to evaluate the ability of E171 particles to promote  
45 conformational changes in amylase and pepsin. Fluorescence emission spectra of  $\alpha$ -amylase and  
46 pepsin was measured in the absence and presence of E171 (Figures 4A and C). The emission peak  
47 observed around 350 nm was assigned to the tryptophan residues located in the protein interior.<sup>61</sup>  
48  
49  
50  
51  
52  
53  
54  
55  
56  
57  
58  
59  
60

1  
2  
3 The fluorescence intensity of  $\alpha$ -amylase and pepsin was quenched substantially by E171 addition.  
4  
5 This quenching effect is consistent with a strong interaction between E171 and the tryptophan  
6  
7 groups of the enzymes.<sup>44</sup> This interaction may have been from hydrogen bonding or hydrophobic  
8  
9 attraction between the E171 and enzymes, leading to a modification in the microenvironment of  
10  
11 the tryptophan groups.  
12  
13

14  
15 The quenching effect of E171 on the fluorescence intensity of  $\alpha$ -amylase and pepsin was  
16  
17 concentration-dependent as described by the Stern-Volmer relation. A linear relationship between  
18  
19  $F_0/F$  of  $\alpha$ -amylase or pepsin and E171(Q) was evident (Figure 4B and D), which is consistent with  
20  
21 previous studies.<sup>42, 44</sup> The mechanisms of fluorescence quenching include dynamic quenching and  
22  
23 static quenching, where the former involves the excited fluorophore quenched upon collision with  
24  
25 a quencher molecule in solution, and the latter is due to non-covalent complex formation between  
26  
27 the fluorophore and quencher.<sup>62</sup> The  $K_q$  values, serving as an essential parameter for the efficiency  
28  
29 of quenching or the availability of the fluorophore to the quencher, derived from the plots of  $F_0/F$   
30  
31 versus [Q], are listed in Table S4. The  $K_q$  values can be used to establish whether the quenching  
32  
33 results from the formation of protein-quencher complexes.<sup>63</sup> The  $K_q$  values of E171 with  $\alpha$ -  
34  
35 amylase and pepsin were approximately 50- and 30- fold, respectively, higher than the maximum  
36  
37 constant ( $2 \times 10^{10} \text{ L mol}^{-1} \text{ s}^{-1}$ ) for dynamic quenching.<sup>64</sup> Hence, the high  $K_q$  values obtained in our  
38  
39 study suggest that both  $\alpha$ -amylase and pepsin were statically quenched due to complex formation  
40  
41 with E171. Assuming E171 could bind to a set of equivalent sites on an active enzyme, the binding  
42  
43 constant ( $K_a$ ) and the number of binding sites ( $n$ ) between the quencher and enzymes were  
44  
45 calculated using the Scatchard equation (Table S4). The  $K_a$  value implies the affinity of E171 to  
46  
47 enzymes.<sup>65</sup> Additionally, the value of  $n$  was approximately equal to 1, indicating a single binding  
48  
49 site mode for the interaction between enzymes and E171.  
50  
51  
52  
53  
54  
55  
56  
57  
58  
59  
60



## Conclusion

This study showed that these digestive enzymes promoted the release of minerals from spinach leaves under simulated gastrointestinal conditions (except for Ca). This promotion was mainly attributed to the ability of the enzymes to break down the plant tissue structure. The addition of E171 (above 0.05 wt%) significantly decreased Fe bioaccessibility by about 5%-11% in the oral phase. This effect was attributed to two processes: (1) inhibition of  $\alpha$ -amylase activity by E171 particles and (2) binding of Fe to the surface of E171 particles. In this study,  $\alpha$ -amylase used was from porcine pancreas.  $\alpha$ -Amylases from different sources have considerable similarity in amino acid sequence.<sup>66</sup> In addition, Pajic et al. found that animals (such as mice, rats, pigs and dogs) that have lived closely with people for centuries, consume a large amount of starch, similar to human food.<sup>67</sup> X-ray crystallography has been used to visualize 3D structures of  $\alpha$ -amylase enzymes from human pancreas and saliva, and from porcine pancreas, both of which are closely related.<sup>68</sup> Previous studies also suggested that both human salivary and pancreatic  $\alpha$ -amylase are similar to rat pancreatic  $\alpha$ -amylases, especially similar to porcine pancreas.<sup>69, 70</sup> Thus, the finding of inhibitory effect of E171 on amylase activity could be extrapolated to human, or is informative for future *in vivo* studies. Fe is an essential element that participates in hundred enzymatic reactions, and Fe deficiency is a global health problem that can cause anemia and immune system disorders. Vegetables are the major sources of vitamins, minerals, and dietary fibers for the human diet. Thus, the significant decrease of Fe bioaccessibility may cause health problems. It has been reported that metal oxide nanoparticles, i.e., CuO, Fe<sub>2</sub>O<sub>3</sub>, and TiO<sub>2</sub>, could alter peanut crop yield as well as nutritional quality such as amino acid, fatty acid profile<sup>71</sup>; exposure to TiO<sub>2</sub> nanoparticles disturbed antioxidant defense system in rice, and also inhibited carbohydrate synthesis, thereby decreased crop yield and quality<sup>72</sup>; cucumber fruit treated with TiO<sub>2</sub> nanoparticles exhibited macromolecule

1  
2  
3 modification, including amide, lignin, and carbohydrates.<sup>73</sup> Most previous studies have been  
4 focused on the effect of TiO<sub>2</sub> nanoparticles on the physiological response and nutritional quality  
5 of crop and implied that TiO<sub>2</sub> could be introduced into the food chain via accumulation in the plant  
6 tissue. However, the information about TiO<sub>2</sub> exposure to the human gastrointestinal tract through  
7 food additives and its impact on nutrient absorption for humans is limited when co-ingested with  
8 vegetables. The results of this study enhance our understanding of the impact of E171 on the  
9 performance of digestive enzymes within the GIT and the nutritional profile of foods. Also, the  
10 findings provide valuable information to guide the development and use of mineral-fortified food  
11 and supplements when E171 is involved.  
12  
13  
14  
15  
16  
17  
18  
19  
20  
21  
22

### 23 **Associated Contents**

24 Supporting information include four tables and two figures.  
25  
26

### 27 **Acknowledgments**

28 The work is supported by USDA NIFA Hatch Program (MAS00549 and CONH00147) and the  
29 Program for Guangdong Introducing Innovative and Entrepreneurial Teams (2019ZT08L213).  
30  
31 Chunyang Li thanks the China Scholarship Council for her study at the University of  
32 Massachusetts (UMass), Amherst, and Baoshan Xing acknowledges the UMass Amherst Conti  
33  
34  
35  
36  
37  
38  
39  
40  
41 Faculty Fellowship.  
42  
43  
44  
45  
46  
47  
48  
49  
50  
51  
52  
53  
54  
55  
56  
57  
58  
59  
60

## References

1. W. Dufou, H. Terrisse, M. Richard-Plouet, E. Gautron, F. Popa, B. Humbert and M. H. Ropers, Criteria to define a more relevant reference sample of titanium dioxide in the context of food: a multiscale approach, *Food Addit. Contam. Part A Chem. Anal. Control Expo. Risk Assess.*, 2017, **34**, 653-665.
2. G. Pinget, J. Tan, B. Janac, N. O. Kaakoush, A. S. Angelatos, J. O'Sullivan, Y. C. Koay, F. Sierro, J. Davis, S. K. Divakarla, D. Khanal, R. J. Moore, D. Stanley, W. Chrzanowski and L. Macia, Impact of the food additive titanium dioxide (E171) on gut microbiota-host interaction, *Front. Nutr.*, 2019, **6**, 57.
3. Z. Chen, Y. Wang, L. Zhuo, S. Chen, L. Zhao, X. Luan, H. Wang and G. Jia, Effect of titanium dioxide nanoparticles on the cardiovascular system after oral administration, *Toxicol. Lett.*, 2015, **239**, 123-130.
4. E. Baranowska-Wojcik, D. Sz wajgier, P. Oleszczuk and A. Winiarska-Mieczan, Effects of titanium dioxide nanoparticles exposure on human health-a review, *Biol. Trace Elem. Res.*, 2020, **193**, 118-129.
5. A. Weir, P. Westerhoff, L. Fabricius, K. Hristovski and N. von Goetz, Titanium dioxide nanoparticles in food and personal care products, *Environ. Sci. Technol.*, 2012, **46**, 2242-2250.
6. EFSA Panel on Food Additives and Nutrient Sources added to Food (ANS), Re-evaluation of titanium dioxide (E171) as a food additive, *EFSA J.*, 2016, **14**, e04545.
7. M. Dorier, D. Béal, C. Tisseyre, C. Marie-Desvergne, M. Dubosson, F. Barreau, E. Houdeau, N. Herlin-Boime, T. Rabilloud and M. Carriere, The food additive E171 and titanium dioxide nanoparticles indirectly alter the homeostasis of human intestinal epithelial cells in vitro, *Environ. Sci.: Nano*, 2019, **6**, 1549-1561.

- 1  
2  
3 8. S. Fiorito, F. Preziuso, F. Epifano, L. Scotti, T. Bucciarelli, V. A. Taddeo and S. Genovese,  
4  
5 Novel biologically active principles from spinach, goji and quinoa, *Food Chem.*, 2019, **276**, 262-  
6  
7 265.  
8  
9
- 10 9. J. L. Roberts and R. Moreau, Functional properties of spinach (*Spinacia oleracea L.*)  
11  
12 phytochemicals and bioactives, *Food Funct.*, 2016, **7**, 3337-3353.  
13  
14
- 15 10. L. I. Elvira-Torales, M. J. Periago, R. Gonzalez-Barrio, N. Hidalgo, I. Navarro-Gonzalez, C.  
16  
17 Gomez-Gallego, D. Masuero, E. Soini, U. Vrhovsek and F. J. Garcia-Alonso, Spinach  
18  
19 consumption ameliorates the gut microbiota and dislipaemia in rats with diet-induced non-  
20  
21 alcoholic fatty liver disease (NAFLD), *Food Funct.*, 2019, **10**, 2148-2160.  
22  
23
- 24 11. K. O. Soetan, C. O. Olaiya and O. E. Oyewole, The importance of mineral elements for  
25  
26 humans, domestic animals and plants: A review, *Afr. J. Food Sci.*, 2010, **4**, 200-222.  
27  
28
- 29 12. M. A. Zoroddu, J. Aaseth, G. Crisponi, S. Medici, M. Peana and V. M. Nurchi, The essential  
30  
31 metals for humans: a brief overview, *J. Inorg. Biochem.*, 2019, **195**, 120-129.  
32  
33
- 34 13. L. Mezzaroba, D. F. Alfieri, A. N. Colado Simao and E. M. Vissoci Reiche, The role of zinc,  
35  
36 copper, manganese and iron in neurodegenerative diseases, *Neurotoxicology*, 2019, **74**, 230-241.  
37  
38
- 39 14. A. Espinoza, S. Le Blanc, M. Olivares, F. Pizarro, M. Ruz and M. Arredondo, Iron, copper,  
40  
41 and zinc transport: inhibition of divalent metal transporter 1 (*DMT1*) and human copper transporter  
42  
43 1 (*hCTR1*) by shRNA, *Biol. Trace Elem. Res.*, 2012, **146**, 281-286.  
44  
45
- 46 15. D. B. Kumssa, E. J. Joy, E. L. Ander, M. J. Watts, S. D. Young, S. Walker and M. R. Broadley,  
47  
48 Dietary calcium and zinc deficiency risks are decreasing but remain prevalent, *Sci. Rep.*, 2015, **5**,  
49  
50 10974.  
51  
52
- 53 16. R. A. Wapnir, Zinc deficiency, malnutrition and the gastrointestinal tract, *J. Nutr.*, 2000, **130**,  
54  
55 1388S-1392S.  
56  
57  
58  
59  
60

- 1  
2  
3 17. L. M. Pompano and J. D. Haas, Increasing iron status through dietary supplementation in iron-  
4 depleted, sedentary women increases endurance performance at both near-maximal and  
5 submaximal exercise intensities, *J. Nutr.*, 2019, **149**, 231-239.  
6  
7  
8  
9  
10 18. E. A. Menezes, A. F. Oliveira, C. J. Franca, G. B. Souza and A. R. A. Nogueira,  
11 Bioaccessibility of Ca, Cu, Fe, Mg, Zn, and crude protein in beef, pork and chicken after thermal  
12 processing, *Food Chem.*, 2018, **240**, 75-83.  
13  
14  
15  
16  
17 19. M. Celus, C. Kyomugasho, L. Salvia-Trujillo, J. Van Audenhove, A. M. Van Loey, T.  
18 Grauwet and M. E. Hendrickx, Interactions between citrus pectin and Zn<sup>2+</sup> or Ca<sup>2+</sup> and associated  
19 in vitro Zn<sup>2+</sup> bioaccessibility as affected by degree of methylesterification and blockiness, *Food*  
20 *Hydrocoll.*, 2018, **79**, 319-330.  
21  
22  
23  
24  
25  
26 20. S. Rousseau, C. Kyomugasho, M. Celus, N. Yeasmen, M. E. Hendrickx and T. Grauwet, Zinc  
27 bioaccessibility is affected by the presence of calcium ions and degree of methylesterification in  
28 pectin-based model systems, *Food Hydrocoll.*, 2019, **90**, 206-215.  
29  
30  
31  
32  
33 21. R. A. de Wijk, J. F. Prinz, L. Engelen and H. Weenen, The role of alpha-amylase in the  
34 perception of oral texture and flavour in custards, *Physiol. Behav.*, 2004, **83**, 81-91.  
35  
36  
37  
38 22. L. Zhao, S. M Budge, A. E Ghaly and M. S Brooks, Extraction, purification and  
39 characterization of fish pepsin: A critical review, *J. Food Process. Technol.*, 2011, **02**.  
40  
41  
42  
43 23. A. Salhi, S. Amara, P. Mansuelle, R. Puppo, R. Lebrun, B. Gontero, A. Aloulou and F.  
44 Carriere, Characterization of all the lipolytic activities in pancreatin and comparison with porcine  
45 and human pancreatic juices, *Biochimie*, 2019, **169**, 106-120.  
46  
47  
48  
49 24. A. Marquez, K. Kocsis, G. Zickler, G. R. Bourret, A. Feinle, N. Husing, M. Himly, A. Duschl,  
50 T. Berger and O. Diwald, Enzyme adsorption-induced activity changes: a quantitative study on  
51 TiO<sub>2</sub> model agglomerates, *J. Nanobiotechnology*, 2017, **15**, 55.  
52  
53  
54  
55  
56  
57  
58  
59  
60

- 1  
2  
3 25. W. Fan, T. Liu, X. Li, R. Peng and Y. Zhang, Nano-TiO<sub>2</sub> affects Cu speciation, extracellular  
4 enzyme activity, and bacterial communities in sediments, *Environ. Pollut.*, 2016, **218**, 77-85.  
5  
6  
7 26. H. Schug, C. W. Isaacson, L. Sigg, A. A. Ammann and K. Schirmer, Effect of TiO<sub>2</sub>  
8 nanoparticles and UV radiation on extracellular enzyme activity of intact heterotrophic biofilms,  
9  
10  
11  
12 *Environ. Sci. Technol.*, 2014, **48**, 11620-11628.  
13  
14 27. R. R. Zhu, W. R. Wang, X. Y. Sun, H. Liu and S. L. Wang, Enzyme activity inhibition and  
15 secondary structure disruption of nano-TiO<sub>2</sub> on pepsin, *Toxicol. In Vitro*, 2010, **24**, 1639-1647.  
16  
17  
18 28. M. Li, Z. Luo, Y. Yan, Z. Wang, Q. Chi, C. Yan and B. Xing, Arsenate accumulation,  
19 distribution, and toxicity associated with titanium dioxide nanoparticles in *Daphnia magna*,  
20  
21  
22  
23 *Environ. Sci. Technol.*, 2016, **50**, 9636-9643.  
24  
25 29. C. Tan and W. X. Wang, Influences of TiO<sub>2</sub> nanoparticles on dietary metal uptake in *Daphnia*  
26  
27  
28  
29 *magna*, *Environ. Pollut.*, 2017, **231**, 311-318.  
30  
31 30. J. Hua, W. J. G. M. Peijnenburg and M. G. Vijver, TiO<sub>2</sub> nanoparticles reduce the effects of  
32  
33  
34 ZnO nanoparticles and Zn ions on zebrafish embryos (*Danio rerio*), *NanoImpact*, 2016, **2**, 45-53.  
35  
36 31. W. Fan, M. Cui, H. Liu, C. Wang, Z. Shi, C. Tan and X. Yang, Nano-TiO<sub>2</sub> enhances the  
37  
38  
39 toxicity of copper in natural water to *Daphnia magna*, *Environ. Pollut.*, 2011, **159**, 729-734.  
40  
41 32. C. Tan, W. H. Fan and W. X. Wang, Role of titanium dioxide nanoparticles in the elevated  
42  
43  
44  
45 uptake and retention of cadmium and zinc in *Daphnia magna*, *Environ. Sci. Technol.*, 2012, **46**,  
46  
47  
48 469-476.  
49  
50 33. A. Brodkorb, L. Egger, M. Alminger, P. Alvito, R. Assuncao, S. Ballance, T. Bohn, C.  
51  
52  
53  
54 Bourlieu-Lacanal, R. Boutrou, F. Carriere, A. Clemente, M. Corredig, D. Dupont, C. Dufour, C.  
55  
56  
57  
58 Edwards, M. Golding, S. Karakaya, B. Kirkhus, S. Le Feunteun, U. Lesmes, A. Macierzanka, A.  
59  
60 R. Mackie, C. Martins, S. Marze, D. J. McClements, O. Menard, M. Minekus, R. Portmann, C. N.

1  
2  
3 Santos, I. Souchon, R. P. Singh, G. E. Vegarud, M. S. J. Wickham, W. Weitschies and I. Recio,  
4 INFOGEST static in vitro simulation of gastrointestinal food digestion, *Nat. Protoc.*, 2019, **14**,  
5 991-1014.  
6  
7

8  
9  
10 34. Y. Li, M. Hu and D. J. McClements, Factors affecting lipase digestibility of emulsified lipids  
11 using an *in vitro* digestion model: proposal for a standardised pH-stat method, *Food Chem.*, 2011,  
12 **126**, 498-505.  
13  
14

15  
16  
17 35. Q. Li, T. Li, C. Liu, G. DeLoid, G. Pyrgiotakis, P. Demokritou, R. Zhang, H. Xiao and D. J.  
18 McClements, Potential impact of inorganic nanoparticles on macronutrient digestion: titanium  
19 dioxide nanoparticles slightly reduce lipid digestion under simulated gastrointestinal conditions,  
20 *Nanotoxicology*, 2017, **11**, 1087-1101.  
21  
22  
23

24  
25  
26 36. W. Wu, R. Zhang, D. J. McClements, B. Chefetz, T. Polubesova and B. Xing, Transformation  
27 and speciation analysis of silver nanoparticles of dietary supplement in simulated human  
28 gastrointestinal tract, *Environ. Sci. Technol.*, 2018, **52**, 8792-8800.  
29  
30  
31

32  
33 37. Z. Wang, J. Zhao, L. Song, H. Mashayekhi, B. Chefetz and B. Xing, Adsorption and  
34 desorption of phenanthrene on carbon nanotubes in simulated gastrointestinal fluids, *Environ. Sci.*  
35 *Technol.*, 2011, **45**, 6018-6024.  
36  
37  
38

39  
40 38. M. Minekus, M. Alminger, P. Alvito, S. Ballance, T. Bohn, C. Bourlieu, F. Carriere, R.  
41 Boutrou, M. Corredig, D. Dupont, C. Dufour, L. Egger, M. Golding, S. Karakaya, B. Kirkhus, S.  
42 Le Feunteun, U. Lesmes, A. Macierzanka, A. Mackie, S. Marze, D. J. McClements, O. Menard, I.  
43 Recio, C. N. Santos, R. P. Singh, G. E. Vegarud, M. S. Wickham, W. Weitschies and A. Brodkorb,  
44 A standardised static in vitro digestion method suitable for food-an international consensus, *Food*  
45 *Funct.*, 2014, **5**, 1113-1124.  
46  
47  
48  
49  
50  
51  
52  
53  
54  
55  
56  
57  
58  
59  
60

- 1  
2  
3 39. D. J. McClements, Enhanced delivery of lipophilic bioactives using emulsions: a review of  
4 major factors affecting vitamin, butraceutical, and lipid bioaccessibility, *Food Funct.*, 2018, **9**, 22-  
5  
6 41.  
7  
8  
9  
10 40. K. Liu, J. Zheng, X. Wang and F. Chen, Effects of household cooking processes on mineral,  
11 vitamin B, and phytic acid contents and mineral bioaccessibility in rice, *Food Chem.*, 2019, **280**,  
12  
13 59-64.  
14  
15  
16  
17 41. S. Jiang, M. Li, R. Chang, L. Xiong and Q. Sun, In vitro inhibition of pancreatic alpha-amylase  
18 by spherical and polygonal starch nanoparticles, *Food Funct.*, 2018, **9**, 355-363.  
19  
20  
21 42. Y. Yue, Z. Wang, Y. Zhang, Z. Wang, Q. Lv and J. Liu, Binding of triclosan and triclocarban  
22 to pepsin: DFT, spectroscopic and dynamic simulation studies, *Chemosphere*, 2019, **214**, 278-287.  
23  
24  
25  
26 43. P. Terra Gde, M. Vinicius De Farias, M. G. Trevisan and J. S. Garcia, Evaluation of pancreatin  
27 stability through enzyme activity determination, *Acta Pharm.*, 2016, **66**, 423-431.  
28  
29  
30  
31 44. Y. Zheng, W. Yang, W. Sun, S. Chen, D. Liu, X. Kong, J. Tian and X. Ye, Inhibition of  
32 porcine pancreatic  $\alpha$ -amylase activity by chlorogenic acid, *J. Funct. Foods*, 2020, **64**, 103587.  
33  
34  
35 45. P. Eck, Recombinant DNA technologies in food, *Biochemistry of Food*, Elsevier, 2013.  
36  
37  
38 46. E. Bala, S. Singha and S. Patra, Polysaccharides from leafy vegetables: chemical, nutritional  
39 and medicinal properties, *Natural Polysaccharides in Drug Delivery and Biomedical Applications*,  
40  
41 2019.  
42  
43  
44 47. L. Taiz; and E. Zeiger, *Plant Physiology*, Sinauer Associates, Inc., Publishers, 2006.  
45  
46  
47 48. Benway Denise A. and C. M. Weaver., Assessing chemical form of calcium in wheat, spinach,  
48 and kale, *J. Food Sci. Technol.*, 1993, **58**, 605-608.  
49  
50  
51  
52  
53  
54  
55  
56  
57  
58  
59  
60



- 1  
2  
3 49. J. C. Allen, J. Y. Issa and W. Cai, Calcium content, in vitro digestibility, and bioaccessibility  
4 in leaves of spinach (*Spinacia oleracea*), sweet potato (*Ipomea batatas*), and drumstick tree  
5 (*Moringa oleifera*), *F1000Research*, 2014, **3**, 65.  
6  
7  
8  
9  
10 50. H. Wang, X. Zhao, X. Han, Z. Tang, S. Liu, W. Guo, C. Deng, Q. Guo, H. Wang, F. Wu, X.  
11 Meng and J. P. Giesy, Effects of monovalent and divalent metal cations on the aggregation and  
12 suspension of Fe<sub>3</sub>O<sub>4</sub> magnetic nanoparticles in aqueous solution, *Sci. Total Environ.*, 2017, **586**,  
13 817-826.  
14  
15  
16  
17  
18  
19 51. M. Karimi, S. Abdolrahimi and G. Pazuki, Bioconjugation of enzyme with silica  
20 microparticles: a promising platform for  $\alpha$ -amylase partitioning, *RSC Advances*, 2019, **9**, 18217-  
21 18221.  
22  
23  
24  
25  
26 52. I. A. Mudunkotuwa and V. H. Grassian, Biological and environmental media control oxide  
27 nanoparticle surface composition: the roles of biological components (proteins and amino acids),  
28 inorganic oxyanions and humic acid, *Environ. Sci.: Nano*, 2015, **2**, 429-439.  
29  
30  
31  
32  
33 53. V. Ernest, G. Sekar, A. Mukherjee and N. Chandrasekaran, Studies on the effect of AgNP  
34 binding on  $\alpha$ -amylase structure of porcine pancreas and *Bacillus subtilis* by multi-spectroscopic  
35 methods, *J. Lumin.*, 2014, **146**, 263-268.  
36  
37  
38  
39  
40 54. E. J. Vernon-Carter, J. Alvarez-Ramirez, M. Meraz and S. Garcia-Diaz, Gaining insights into  
41 alphaamylase inhibition by glucose through mathematical modeling and analysis of the hydrolysis  
42 kinetics of gelatinized corn starch dispersions, *Int. J. Biol. Macromol.*, 2019, **132**, 766-771.  
43  
44  
45  
46  
47 55. R. Arunkumar, C. J. Drummond and T. L. Greaves, FTIR spectroscopic study of the secondary  
48 structure of globular proteins in aqueous protic ionic liquids, *Front Chem.*, 2019, **7**, 74.  
49  
50  
51  
52  
53  
54  
55  
56  
57  
58  
59  
60

- 1  
2  
3 56. J. Wu, X. Guo, H. Liu and L. Chen, Isolation and comparative study on the characterization  
4 of guanidine hydrochloride soluble collagen and pepsin soluble collagen from the body of surf  
5 clam shell (*Coelomactra antiquata*), *Foods*, 2019, **8**.  
6  
7  
8  
9  
10 57. H. K. Al-Hakeim and K. M. Jasem, High ionic strength enhances the nnti-pepsin activity of  
11 titanium dioxide nanoparticles, *Nano Biomed. Eng.*, 2016, **8**.  
12  
13  
14 58. F. Secundo, Conformational changes of enzymes upon immobilisation, *Chem. Soc. Rev.*, 2013,  
15 **42**, 6250-6261.  
16  
17  
18  
19 59. A. M. Pascoal, S. Mitidieri and K. F. Fernandes, Immobilisation of  $\alpha$ -amylase from  
20 *Aspergillus niger* onto polyaniline, *Food Bioprod. Process.*, 2011, **89**, 300-306.  
21  
22  
23 60. W. Jin, Z. Wang, D. Peng, W. Shen, Z. Zhu, S. Cheng, B. Li and Q. Huang, Effect of pulsed  
24 electric field on assembly structure of  $\alpha$ -amylase and pectin electrostatic complexes, *Food*  
25 *Hydrocoll.*, 2020, **101**, 105547.  
26  
27  
28  
29 61. J. T. Vivian and P. R. Callis, Mechanisms of tryptophan fluorescence shifts in proteins,  
30 *Biophys. J.*, 2001, **80**, 2093-2109.  
31  
32  
33  
34 62. X. Cai, J. Yu, L. Xu, R. Liu and J. Yang, The mechanism study in the interactions of sorghum  
35 procyanidins trimer with porcine pancreatic alpha-amylase, *Food Chem.*, 2015, **174**, 291-298.  
36  
37  
38  
39 63. L. Sun, W. Chen, Y. Meng, X. Yang, L. Yuan, Y. Guo, F. J. Warren and M. J. Gidley,  
40 Interactions between polyphenols in thinned young apples and porcine pancreatic alpha-amylase:  
41 Inhibition, detailed kinetics and fluorescence quenching, *Food Chem.*, 2016, **208**, 51-60.  
42  
43  
44  
45 64. G. Zhang and Y. Ma, Mechanistic and conformational studies on the interaction of food dye  
46 amaranth with human serum albumin by multispectroscopic methods, *Food Chem.*, 2013, **136**,  
47 442-449.  
48  
49  
50  
51  
52  
53  
54  
55  
56  
57  
58  
59  
60

- 1  
2  
3 65. M. Miao, B. Jiang, H. Jiang, T. Zhang and X. Li, Interaction mechanism between green tea  
4 extract and human alpha-amylase for reducing starch digestion, *Food Chem.*, 2015, **186**, 20-25.  
5  
6  
7 66. B. C. Pang and B. K. Cheung, Applicability of two commercially available kits for forensic  
8 identification of saliva stains, *J. Forensic. Sci.*, 2008, **53**, 1117-1122.  
9  
10  
11 67. P. Pajic, P. Pavlidis, K. Dean, L. Neznanova, R. A. Romano, D. Garneau, E. Daugherity, A.  
12 Globig, S. Ruhl and O. Gokcumen, Independent amylase gene copy number bursts correlate with  
13 dietary preferences in mammals, *Elife*, 2019, **8**.  
14  
15  
16 68. P. J. Butterworth, F. J. Warren and P. R. Ellis, Human  $\alpha$ -amylase and starch digestion: An  
17 interesting marriage, *Starch-Stärke*, 2011, **63**, 395-405.  
18  
19  
20 69. S. Janecek, Sequence similarities and evolutionary relationships of microbial, plant and  
21 animal  $\alpha$ -amylases, *Eur. J. Biochem.*, 1994, **224**, 519-524.  
22  
23  
24 70. N. Ramasubbu, V. Paloth, Y. Luo, G. D. Brayer and M. J. Levine, Structure of human salivary  
25 alpha-amylase at 1.6 Å resolution: implications for its role in the oral cavity, *Acta Crystallogr.*,  
26 1996, **52**, 435-446.  
27  
28  
29 71. M. Rui, C. Ma, J. C. White, Y. Hao, Y. Wang, X. Tang, J. Yang, F. Jiang, A. Ali, Y. Rui, W.  
30 Cao, G. Chen and B. Xing, Metal oxide nanoparticles alter peanut (*Arachis hypogaea* L.)  
31 physiological response and reduce nutritional quality: a life cycle study, *Environ. Sci.: Nano*, 2018,  
32 **5**, 2088-2102.  
33  
34  
35 72. B. Wu, L. Zhu and X. C. Le, Metabolomics analysis of TiO<sub>2</sub> nanoparticles induced  
36 toxicological effects on rice (*Oryza sativa* L.), *Environ. Pollut.*, 2017, **230**, 302-310.  
37  
38  
39 73. A. D. Servin, M. I. Morales, H. Castillo-Michel, J. A. Hernandez-Viezcas, B. Munoz, L. Zhao,  
40 J. E. Nunez, J. R. Peralta-Videa and J. L. Gardea-Torresdey, Synchrotron verification of TiO<sub>2</sub>  
41  
42  
43  
44  
45  
46  
47  
48  
49  
50  
51  
52  
53  
54  
55  
56  
57  
58  
59  
60

1  
2  
3 accumulation in cucumber fruit: a possible pathway of TiO<sub>2</sub> nanoparticle transfer from soil into  
4  
5 the food chain, *Environ. Sci. Technol.*, 2013, **47**, 11592-11598.  
6  
7  
8  
9  
10  
11  
12  
13  
14  
15  
16  
17  
18  
19  
20  
21  
22  
23  
24  
25  
26  
27  
28  
29  
30  
31  
32  
33  
34  
35  
36  
37  
38  
39  
40  
41  
42  
43  
44  
45  
46  
47  
48  
49  
50  
51  
52  
53  
54  
55  
56  
57  
58  
59  
60

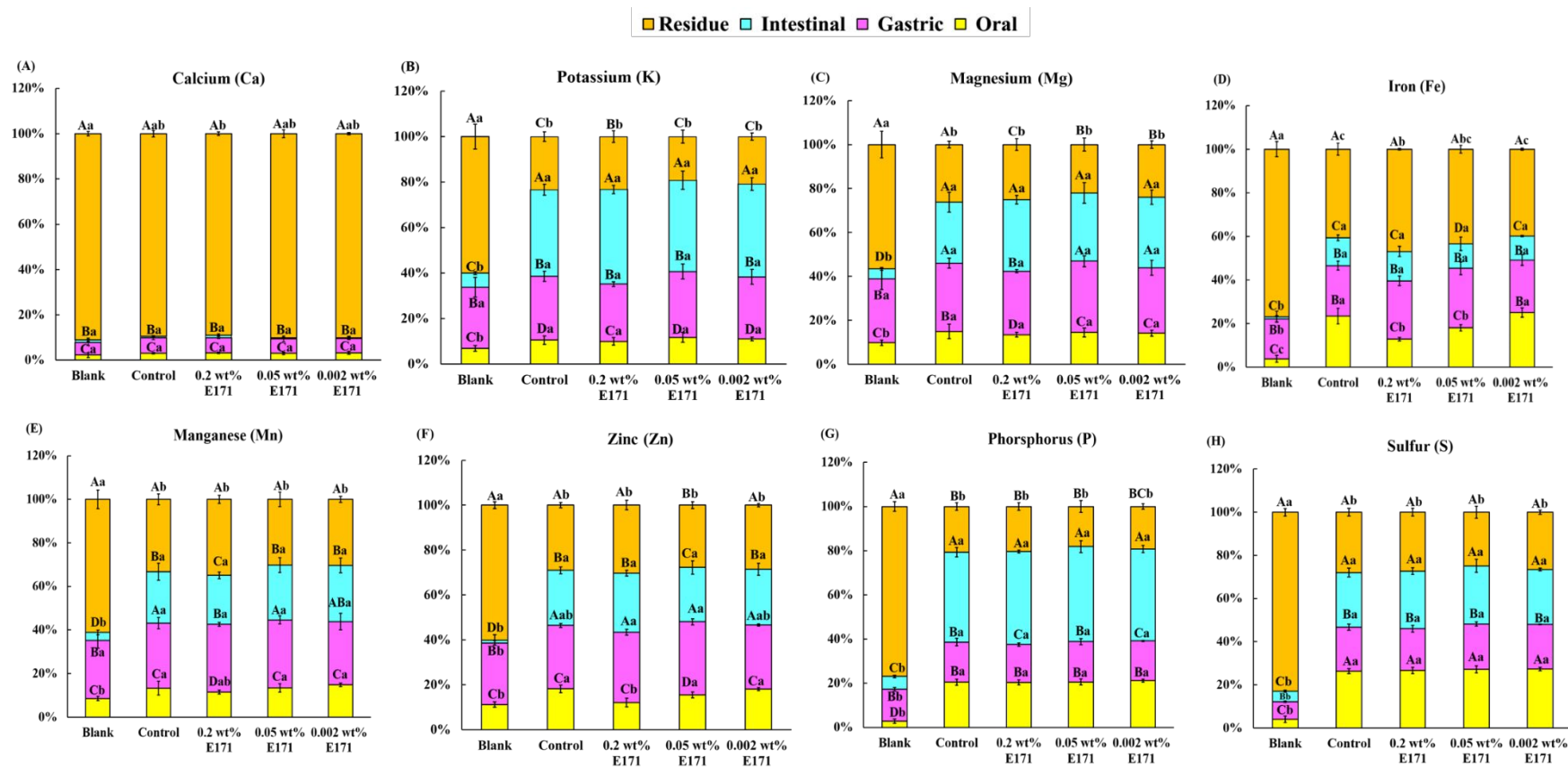


Figure 1. The amount (%) of mineral nutrients (Ca, K, Mg, Fe, Mn, Zn, P, and S) released in the oral, gastric, and small intestinal phase, as well as that remaining in spinach leaves, under 0 (in the absence (blank) or presence (control) of digestive enzymes), 0.002, 0.05, or 0.2 wt% E171. Ca released in the small intestinal is shown in Figure S1. Bars with different uppercase (A-C) are significantly different ( $p < 0.05$ ) when comparing between different regions for the same treatment. Bars with different lowercase letters (a-c) are significantly different ( $p < 0.05$ ) when compared among 0, 0.002, 0.05 and 0.2 wt% E171 in the same region.

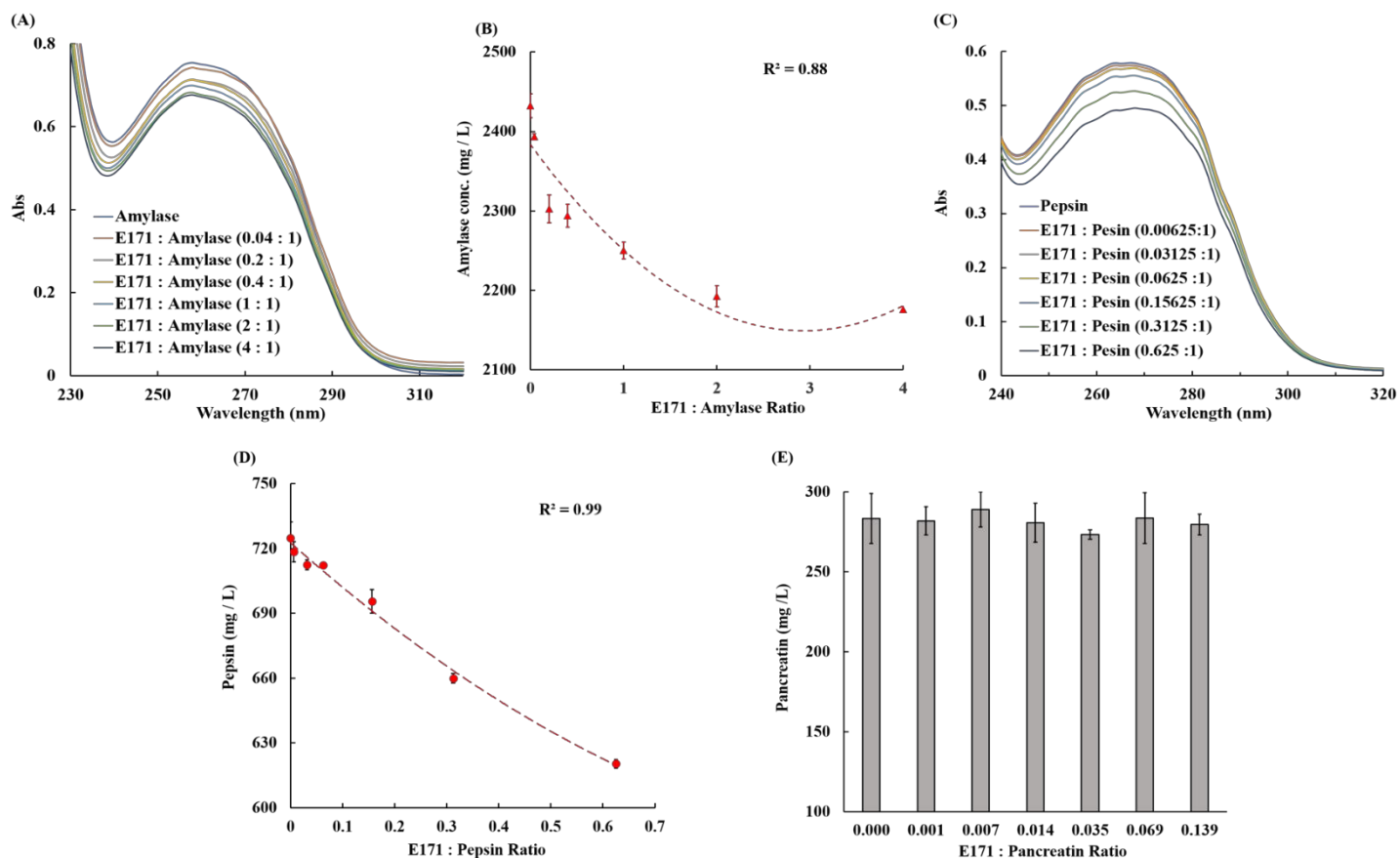


Figure 2. (A) UV-vis spectra of  $\alpha$ -amylase (initial concentration  $5 \text{ mg mL}^{-1}$ ) under various initial concentrations of E171 (0, 0.2, 1, 2, 5, 10, 20  $\text{mg mL}^{-1}$ ) in the oral phase; (B) The correlation ( $R^2 = 0.88$ ) between  $\alpha$ -amylase concentration ( $\text{mg mL}^{-1}$ ) in the supernatant and initial concentration ratio of E171 to  $\alpha$ -amylase (0, 0.04, 0.2, 0.4, 1, 2, 4); (C) UV-vis spectra of pepsin (initial concentration at  $3.2 \text{ mg mL}^{-1}$ ) under various initial concentrations of E171 (0, 0.02, 0.1, 0.2, 0.5, 1, 2  $\text{mg mL}^{-1}$ ) in the gastric phase; (D) The correlation ( $R^2 = 0.99$ ) between pepsin concentration ( $\text{mg mL}^{-1}$ ) in the supernatant and initial concentration ratio of E171 to pepsin (0, 0.00625, 0.03125, 0.0625, 0.15625, 0.3125, 0.625); (E) Pancreatin concentration ( $\text{mg mL}^{-1}$ ) in the supernatant under various initial concentration ratios of E171 to pancreatin (0, 0.001, 0.007, 0.014, 0.035, 0.069, 0.139).

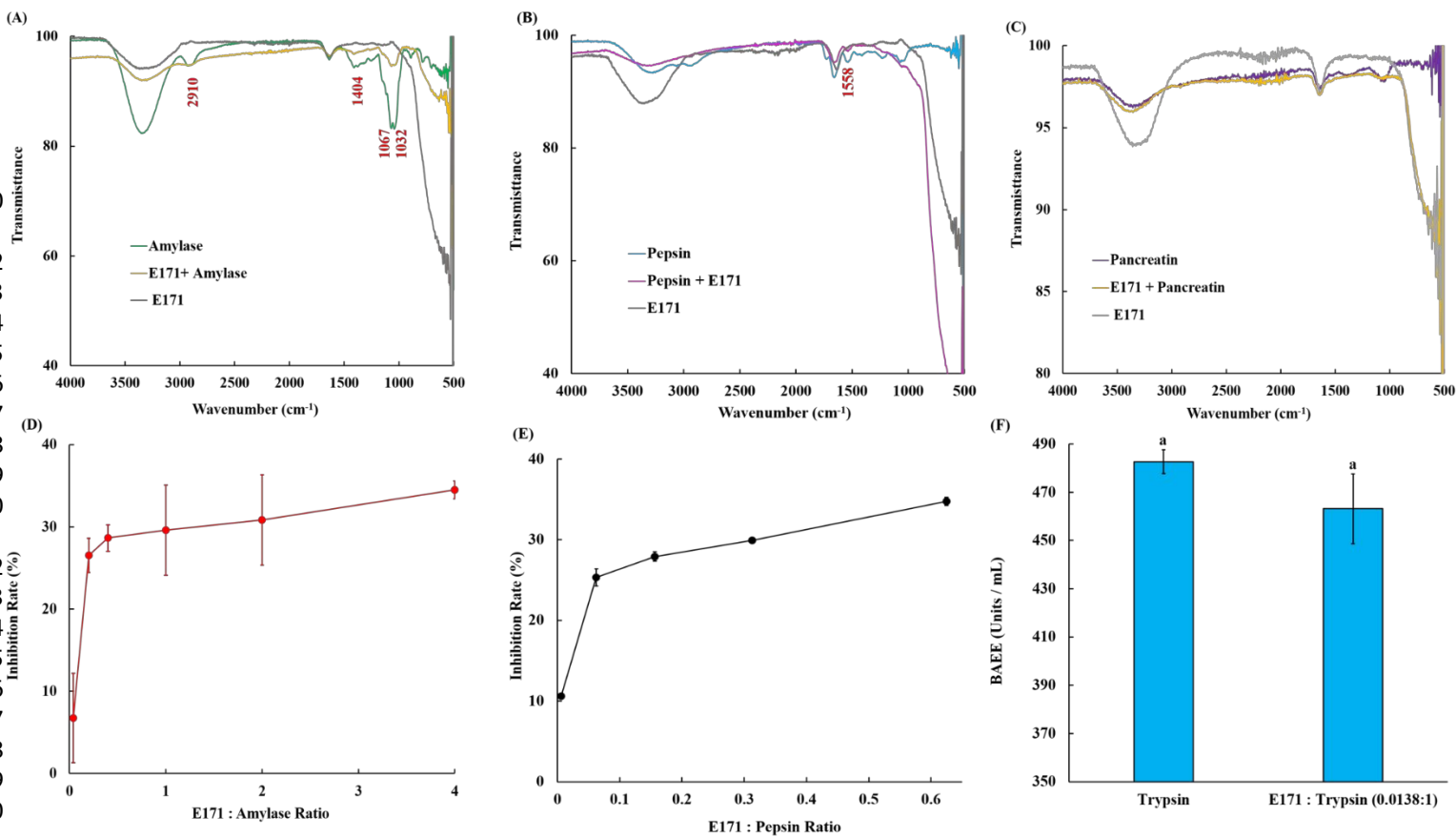


Figure 3. (A) FTIR spectra of  $\alpha$ -amylase, E171,  $\alpha$ -amylase + E171 in the oral phase; (B) FTIR spectra of pepsin, E171, pepsin + E171 in the gastric phase; (C) FTIR spectra of pancreatin, E171, pancreatin + E171 in the small intestinal phase; Inhibitory effects of E171 on (D)  $\alpha$ -amylase activity as affected by E171 in the oral phase; (E) pepsin activity as affected by E171 in the gastric phase; (F) pancreatin activity in the small intestinal phase.

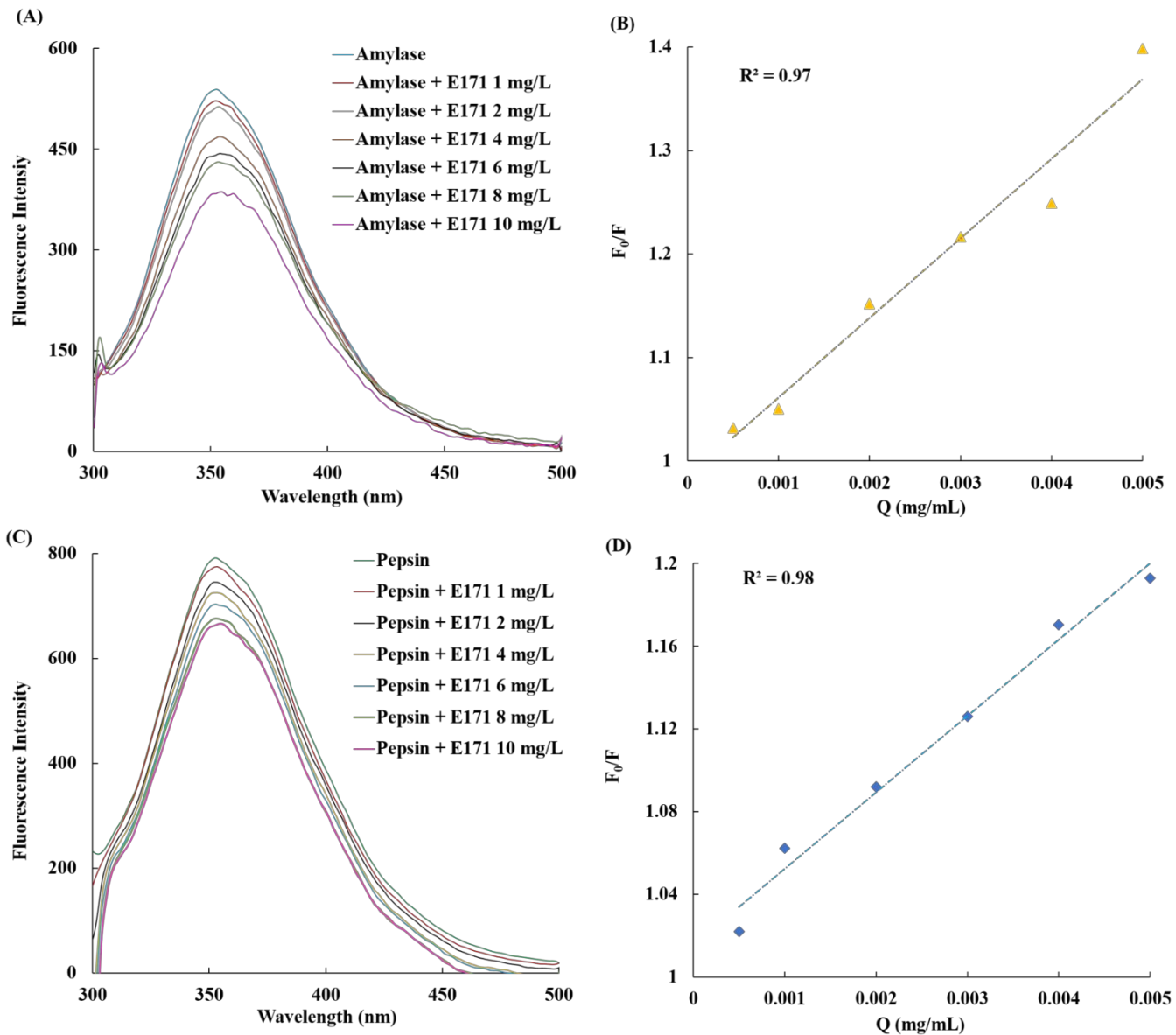


Figure 4. Changes in the intrinsic (A)  $\alpha$ -amylase and (C) pepsin fluorescence at different concentrations of E171 (0-10 mg L<sup>-1</sup>); the Stern-Volmer curves of (B)  $\alpha$ -amylase and (D) pepsin quenched by E171. The initial concentration of  $\alpha$ -amylase and pepsin were 150 and 75 mg L<sup>-1</sup>, respectively.



Table 1. Mineral Adsorption (%) onto 0.2, 0.005, and 0.002 wt% E171 in the oral, gastric, and small intestinal phase. Bars with different capital letters (A-C) are significantly different ( $p < 0.05$ ) when comparing between different regions for a same treatment. Bars with different lower-case letters (a-c) are significantly different ( $p < 0.05$ ) when compared various E171 additions (0.002, 0.05 and 0.2 wt%) in the same region.

		Ca (%)	K (%)	Mg (%)	Fe (%)	Mn (%)	Zn (%)	P (%)	S (%)
Oral Phase	0.2% E171	☐	☐	0.48 ± 0.31	5.30a ± 1.09	4.47Aa ± 0.63	3.66Aa ± 1.20	☐	1.26B ± 0.84
	0.05% E171	☐	☐	☐	3.02b ± 1.08	1.41b ± 0.31	1.60a ± 0.75	☐	☐
	0.002% E171	☐	☐	☐	☐	☐	☐	☐	☐
Gastric Phase	0.2% E171	☐	☐	☐	☐	☐	☐	☐	3.10A ± 1.42
	0.05% E171	☐	☐	☐	☐	☐	☐	☐	☐
	0.002% E171	☐	☐	☐	☐	☐	☐	☐	☐
Small Intestinal Phase	0.2% E171	0.70a ± 0.35	☐	☐	☐	4.01A ± 2.74	4.27A ± 3.35	0.90a ± 0.49	☐
	0.05% E171	0.19b ± 0.16	☐	☐	☐	☐	☐	1.07a ± 0.60	☐
	0.002% E171	☐	☐	☐	☐	☐	☐	☐	☐

“☐” = No measurable mineral adsorbed on E171 particles